Galton-Fenzi, B.K., Scott, W.D., Farrow, D.E. and Handsworth, R. (2006) Revisiting the anomalous shelf water oscillation of Buckles Bay, Macquarie Island. Continental Shelf Research, 26 (19). pp. 2386-2392.

Revisiting the anomalous shelf water oscillation of Buckles Bay, Macquarie Island

B.K.Galton-Fenzi[a]

W.D.Scott[a]

D.E.Farrow[b]

R.Handsworth[c]

[a]School of Environmental Science, Murdoch University, Murdoch, Western Australia, Australia

[b]School of Engineering Science, Murdoch University, Murdoch, Western Australia, Australia

[c]Data Centre, Australian Antarctic Division, Kingston, Tasmania

Abstract

Historic observations of sea-level on Macquarie Island recorded an ∼6min oscillation with a perceived beat of ∼3h, interpreted as two counter-rotating edge waves of slightly different frequencies. Alternative evidence is presented here that the oscillations are consistent with the fundamental shelf period of Buckles Bay; an envelope characteristic of local coast and shelf features. New data from a shore-mounted tide gauge, analyzed using fourier and wavelet techniques, show an ∼6.6min phenomenon occurring in bursts every 1–4 h. A simple model shows that the fundamental resonant frequency may spread and comply with maximum and minimum coast and shelf features.

Keywords: Sea level; Oscillations; Resonance; Frequencies; Coastal; Seiches; Wavelets; Islands; Southern Ocean

1. Introduction

The tide gauges at Macquarie Island are used to investigate and characterize gauge response to sea-level. Of concern are anomalies and local bias in the record and so the gauges currently sample within the 'spectral-valley' so noise and bias are minimized. The 'spectral-valley' is a quiet frequency range between periods of oceanographic activity from minutes to several hours. However, periodic sea-level oscillations occur within this range in many coastal areas. These include shelf oscillations often driven by the open ocean at anomalous periods. Understanding them is important for efficient coastal management such as predicting the local effect of tsunamis and storm surges.

An oscillation with a period of ∼6min was detected in floating G.P.S. buoy data at Macquarie Island about 100 m offshore (Fig. 1) (Watson, 2005). Historical studies from shore mounted tide gauges have shown similar oscillations with a beating amplitude of 3 h (Summerfield, 1967). Specifically the frequency analysis of Summerfield (1967), using three different 5 h periods, suggested the oscillation to be composed of two distinct waves with periods of 6.3 and 6.8 min.

Longuet-Higgins (1967) attempted to account for the two periods by considering counter-rotating waves trapped around a circular island whereby the coriolis force causes the wave propagating with the force to lead, and its counter-rotating twin (propagating against the force) to lag. A three hourly beat then follows; however, it was found that the split was an order of magnitude too small, even allowing for sloping bathymetry Longuet-Higgins (1967). Macquarie Island is not circular; it has an elongated rectangular shape. Further, the observations of Summerfield (1967) were affected by short length and poor spectral resolution (2 DoF) so the wave envelope may not have been properly presented. These considerations suggest the mechanism producing the ∼6min wave needed further investigation.

This paper firstly presents the physical setting, then an alternative mechanism to show how local variations in the coast and shelf can cause a spread in the frequency response. Longer records of more recent data are used to investigate the phenomenon. Changes of spectral energy with time are considered, using fast Fourier transforms (FFTs), following Summerfield (1967). Lastly, a wavelet analysis addresses the limitations of the FFTs when analyzing frequencies with temporal variability to highlight the arrhythmic nature of a resonance period confined to a distinct bandwidth.

2. The physical setting

Macquarie Island (lat.54°30′S, long.158°58′E) is located in the Southern Ocean and is a surface expression of the elongated north–south Macquarie Ridge. Macquarie Island has a narrow shelf (∼100m wide) with a steep drop-off on all sides to the abyssal plain; the lee side (east side) is bracketed by the Hjord Trench (∼6000m deep). The mean water depth at the shelf edge is ∼50m. The shelf width in the vicinity of Buckles Bay is within the range of 900–1300 m. Vertical associations of the minimum and maximum shelf and slopes within Buckles Bay are shown as transects X–Y and X–Z in Fig. 2. The transects are presented in profile on Fig. 3.

3. Shelf resonance

Waves that enter the shelf system are modified by a number of processes. As the depth decreases there is a reduction in speed. To maintain mass and energy balances the wave amplitude must increase (Simpson, 1998). The energy transfer is most effective if the forcing frequency matches the 'natural' shelf resonance.

The 'natural' shelf resonance is dependent on the geometry of the coast and shelf in the simplest sense. That is, the topography determines the resonant frequency f_0 and the spread of the resonant frequency Δf (Wilson, 1972; Simpson, 1998). Traditionally, the spread refers to the peakedness of the wave and can be described by its quality Q, a dimensionless parameter where $Q=f_0/\Delta f$. Q usually represents damping from frictional and edge effects at the boundaries for a perfect rectilinear oscillator; a high Q indicates little energy is lost. The solutions presented here allow that the Δf in the dimensionless parameter Q might also come from a spread of resonant frequencies. Subtle differences in the local topography should have an effect on the path a wave may take and produce such a spread.

3.1. The fundamental shelf period—T_0

A simple model of shelf resonance is a standing wave (Fig. 4a and b) with an antinode at the shoreline and a node at the edge of the shelf. A one-dimensional simple harmonic oscillator describes the motions where the period can be determined using the Du Boys equation (Hutchinson, 1957). The modes of a resonant system differ by the number of nodes but are usually dominated by the fundamental mode T_0. On Fig. 4(b) the period is four times the travel time from the coast (x=0) to the shelf-edge ($x=A$). For a depth h, shallow water wave theory gives the celerity of the wave as

$$c = c(x) = \sqrt{gh}.$$

The period of the fundamental mode T_0 is given by the integral equation (Munk, 1962):

$$T_0 = 4\int_0^A \frac{\mathrm{d}x}{c(x)} = \frac{4A}{\sqrt{g}(H_A - H_0)} \int_{H_0}^{H_A} \frac{\mathrm{d}h}{\sqrt{h}}. \tag{1}$$

For a bottom with a uniform slope $s=(H_A-H_0)/A$,

$$h = h(x) = \left(\frac{H_A - H_0}{A}\right)x + H_0,$$

where H_A is the depth at the shelf position $x=A$; H_0 is the depth at the coast $x=0$. Substituting and simplifying gives,

$$T_0 = \frac{8A}{\sqrt{g}(\sqrt{H_A} + \sqrt{H_0})}. \tag{2}$$

Note that if $H_0 \ll H_A$, this yields the classical expression for travel over a shelf of width A (Munk, 1962).

Further, accepting the limitations of the shallow water equation, the travel time over the sill (width B) is a similar expression,

$$T_{Sill} = \frac{8B}{\sqrt{g}(\sqrt{H_B}+\sqrt{H_A})}. \quad (3)$$

The total time of travel T_T over the sill and shelf is

$$T_T \cong T_0 + T_{Sill} \quad (4)$$

and the frequency of a long-wave passing over the shelf and sill is $f_T=1/T_T$.

3.2. Estimating the bandwidth—Δ*f*

The spread of frequencies considers the variation in travel time over the shelf and sill. Islands are not of rectilinear geometry and waves on a coast may reflect at odd angles at the coast and sill and travel different paths. Here we show variations in T_0 and Δf specific to the local dimensions of Buckles Bay.

One variation in Δf can come from comparing a wave reflected from a steep cliff with one that runs-up a gently sloping beach (an extension of the sloping shelf):

$$Q_{Coast} \simeq \frac{\sqrt{H_A}+\sqrt{H_0}}{\sqrt{H_0}}. \quad (5)$$

Near the location of the tide gauges there is a beach and a nearly vertical rock face with a height of about 5 m. See Fig. 4, left-side, H_0 is ~5m, $H_A \simeq 50$m and Q_{Coast}~3. A gently sloping beach is an efficient ‘trap’ for a specific frequency.

Similarly, the Q estimate for the coastal variation between a sill with a slope and a sill of no slope is

$$Q_{Sill} \simeq \frac{\frac{1}{T_T}}{\frac{1}{T_0} - \frac{1}{T_T}} \quad (6)$$

which, from Eqs. (2), (3) and (6), as B approaches 0, Q approaches infinity. That is, Δf will converge toward one frequency; a steep sill is a trap for a specific frequency. For Macquarie Island, $H_A \simeq 50$m, $H_B \approx 3000$m, $A \simeq 1000$m, $B \approx 3500$m, and, $Q_{Sill} \approx 2$.

A general estimate of maximum and minimum shelf effects can be gained from the long-sections of Figs. 2 and 3. Further analysis following Eq. (1) gives periods 5.2–7.7 min ($\Delta f \sim 0.06$min^{-1} and a $Q \sim 2.5$).

The prediction of the fundamental mode period for coastal oscillations local to Buckles Bay is ∼5–8 min with Q in the range of ∼2–3. This simplest of methods can show the range of frequencies that might be expected due to the local geometry.

4. Data analysis

The Australian Antarctic Division (AAD) pressure tide-gauge at Buckles Bay (TG in insert of Fig. 2) was programmed to acquire one sample every 10 s with each sample consisting of a 10 s integration of pressure centered at the time stamp. Continuous records over 26 days produced 224,640 samples.

The mean and linear trend were removed. A 6 point box-car filter removed periods shorter than 60 s. Low frequencies (>30minperiods) were separated by applying a low-bandpass 30 point raised cosine filter to the 1 min values resulting from the 6 point filter. The final high-pass filtered data set was obtained by subtracting the low-pass data from the 6 point filtered data.

Frequency spectra used segmented sections of the 26 day time series. A single segment consisted of a time series of 1024 points of 1 min data. Each segment was smoothed using a Hanning window with a 50% overlap between segments (Harris, 1978, p. 463). An FFT algorithm was used to calculate the spectra for each of the 72 segments.

4.1. The FFT spectrum

Following Summerfield (1967), the 72 individual frequency spectra showed dominant peaks. A representative sample of nine spectra are presented in Fig. 5. Each spectra was smoothed using a 3 point running box-car average (solid line), with 17 h and 4 min of data per spectrum. Comparing the spectra in Fig. 5 shows a number of different frequencies of varying amplitude. Fig. 5(e and h), for example, suggest something akin to the results of Summerfield. There are not two central peaks, however; the peaks tend to shift in frequency and ‘overlap’.

As an extension of Summerfield's analysis, an average ‘envelope’ of activity is presented in Fig. 6 with a 95% confidence interval. Each point (circle) is the average from the 72 FFTs. The envelope shows rapid fall-off at the high frequency and the lower end has a tail that fades into the background noise. Comparing the envelope with the background noise, at half power, gives an envelope period of 5.7–7.4 min. The averaged spectrum shows three possible peaks; however, the peaks do not exceed the error bars and have little statistical validity.

The individual spectra (Fig. 5) contain non-stationary components and the averaged spectra suggest a major oscillation with some statistical variation (Fig. 6). However, changes in the spectra cannot be observed at periods less than 17.07 h using the FFT technique. The non-stationary nature of the phenomenon requires an analysis that distinguishes the changes and spread of resonant frequencies with time, a method of time-frequency localization, such as wavelet analysis.

4.2. Wavelet analysis

Continuous wavelet analysis generates a localized amplitude and phase for each frequency component and identifies periodic signals in non-stationary data. When adapted, only a narrow time window is needed to examine high-frequency content (Ogden, 1997).

The material by Torrence and Compo (1998) and complimentary software were helpful for the analysis. The results below utilize a Morlet mother wavelet as the wavelet function. Each of the wavelets used 2048 of the 1 min filtered data for a record length of 34.13 h. Inspection confirms the FFT estimation of the spectral width is roughly repeated in the 5% white noise contour (dark solid line) of Fig. 7. The plot indicates episodic yet arrhythmic energy at periods within the ‘natural’ envelope. The beating observed in the wavelet spectra of Fig. 7 is not with great regularity, as presumed by Summerfield (1967).

5. Discussion

The analysis of long tide-gauge records supports shelf resonance at the fundamental mode of oscillation. The model effectively shows how the observed oscillation and the spread of frequencies might occur without dissipation. The ‘beating’ observed by Summerfield may well be caused by ‘new’ energy moving into shelf waters at the shelf resonance frequency.

Individual spectra show multiple peaks, more than two, with shifting amplitudes and frequencies (Fig. 5). The variability observed is supported by the averaged spectra with a higher statistical reliability (Fig. 6). The wavelet analysis highlights the time localized frequency content of the oscillatory envelope local to Buckles Bay in a distinct band of activity. Individual peaks come and go and separate frequencies are undifferentiated.

The observed spread of energy at the fundamental period may arise from three main processes: (1) leakage in the FFT analysis; (2) trapping at near to resonance frequencies; and (3) coastal/topographical effects. In the FFT analysis, the leakage of energy into the band was minimized by effective windowing and the wavelet analysis confirms a distinct band of activity. Trapping at near to a resonant frequency is not likely as it would be one oscillation with a distinct well defined bandwidth.

Here the aim was to demonstrate that including a range of local parameters in a simple model may cause a spread of frequencies due to different across-shelf travel times. In fact the coast is a continuum of irregularities which can contribute to the distortion of the resonant frequency. Shelves with large variation are expected to have a larger bandwidth while uniform rectilinear shelves, with perfect reflection at the coast, can have a well-defined narrow bandwidth. In summary, a simple model of a coastal seiche, for the maximum and minimum shelf features of Buckles Bay, is consistent with the observations.

Acknowledgments

Thanks to Henk Brolsma and the AAD Data Centre, Rolf Koch of Murdoch University, as well as John Hunter and Chris Watson of the University of Tasmania.

References

Emery, W.J., Thomson, R.E., 2001. Data Analysis Methods in Physical Oceanography, second ed. Elsevier, Amsterdam, p. 638

Harris, F.J., 1978. On the use of windows for harmonic analysis with the discrete fourier transform. Proceedings of the IEEE 66, 51–84.

Hutchinson, G.E., 1957. A Treatise on Limnology, vol. 1015. Wiley, New York, p. 540.

Longuet-Higgins, M.S., 1967. On the trapping of wave energy round islands. J. Fluid Mech. 29 (part 4), 781–821.

Munk, W.H., 1962. Long ocean waves. In: Hill, M.N. (Ed.), The Sea, vol. 1. Interscience Publisher, New York, pp. 647–663.

Ogden, R.T., 1997. Essential Wavelets for Statistical Applications and Data Analysis. Birkha¨user, Boston, p. 206.

Simpson, J.H., 1998. Tidal processes in shelf seas. In: Brink, K.H., Robinson, A.R. (Eds.), The Sea, vol. 10. Interscience Publisher, New York, pp. 113–150.

Summerfield, W., 1967. On the six minute period wave phenomenon recorded at Macquarie Island. Horace Lamb Centre for Oceanographic Research Papers, No. 16.

Torrence, C., Compo, G.P., 1998. A practical guide to wavelet analysis. Bulletin of the American Meteorological Society 79 (1), 61–78.

Watson, C.S., 2005. Development of GPS buoy technology for satellite altimeter calibration/verification. Ph.D. Thesis, University of Tasmania.

Wilson, B.W., 1972. Seiches. Advances in Hydroscience 8, 1–94

Fig. 1. Floating buoy power spectra from the shelf seas near Buckles Bay, Macquarie Island; sampled at 1 Hz for 16 h on the 6th March 2003. The arrow indicates the ≈6min periodic event (taken from Watson, 2005).

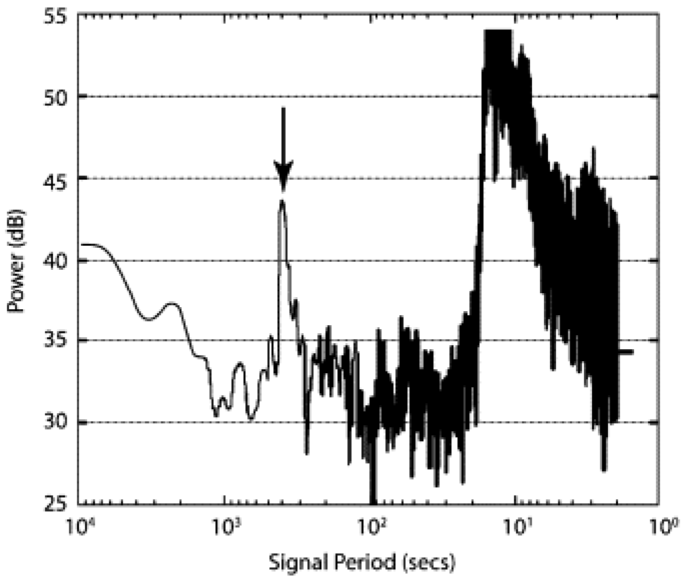

Fig. 2. Buckles Bay cove and Hasselborough Bay, showing the approximate location of two transects (X–Y and X–Z) and the approximate bathymetry. Insert shows the location of the tide gauge, at TG, in Garden Cove. A long-section view of the transects X–Y and X–Zis presented in Fig. 3

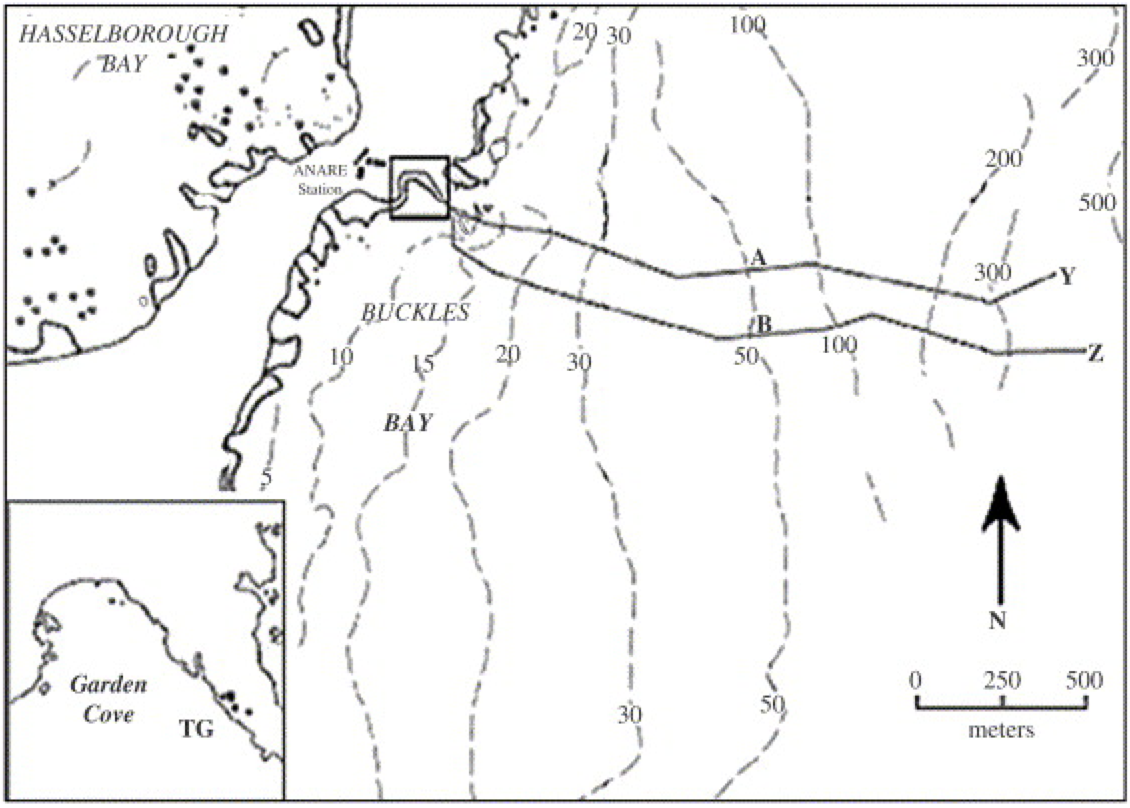

Fig. 3. Vertical long-section view of two possible flow lines (X–Y and X–Z) from Fig. 2. Arrows show the estimates of the shelf edge depth (A and B) for each respective transect; all scales are in meters.

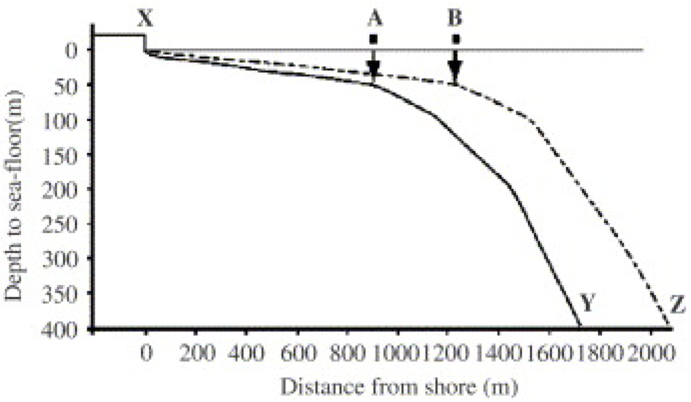

Fig. 4. Shelf oscillations: (a) formation of shelf oscillations by reflection at the coast; (b) idealized bottom profile showing shelf and sill slope characteristics.

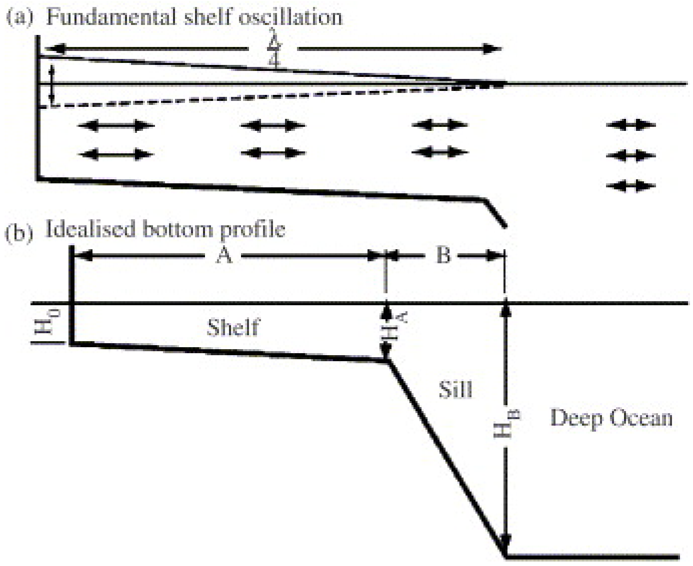

Fig. 5. A sample of nine consecutive series as FFT spectra (points), parts (a)–(i). The solid line is a 3 point average showing variation within 0.17-0.14min^{-1}(DoF=6). Each spectra was analyzed with a 1024 point FFT using 1 min data, beginning year day 154 (2004).

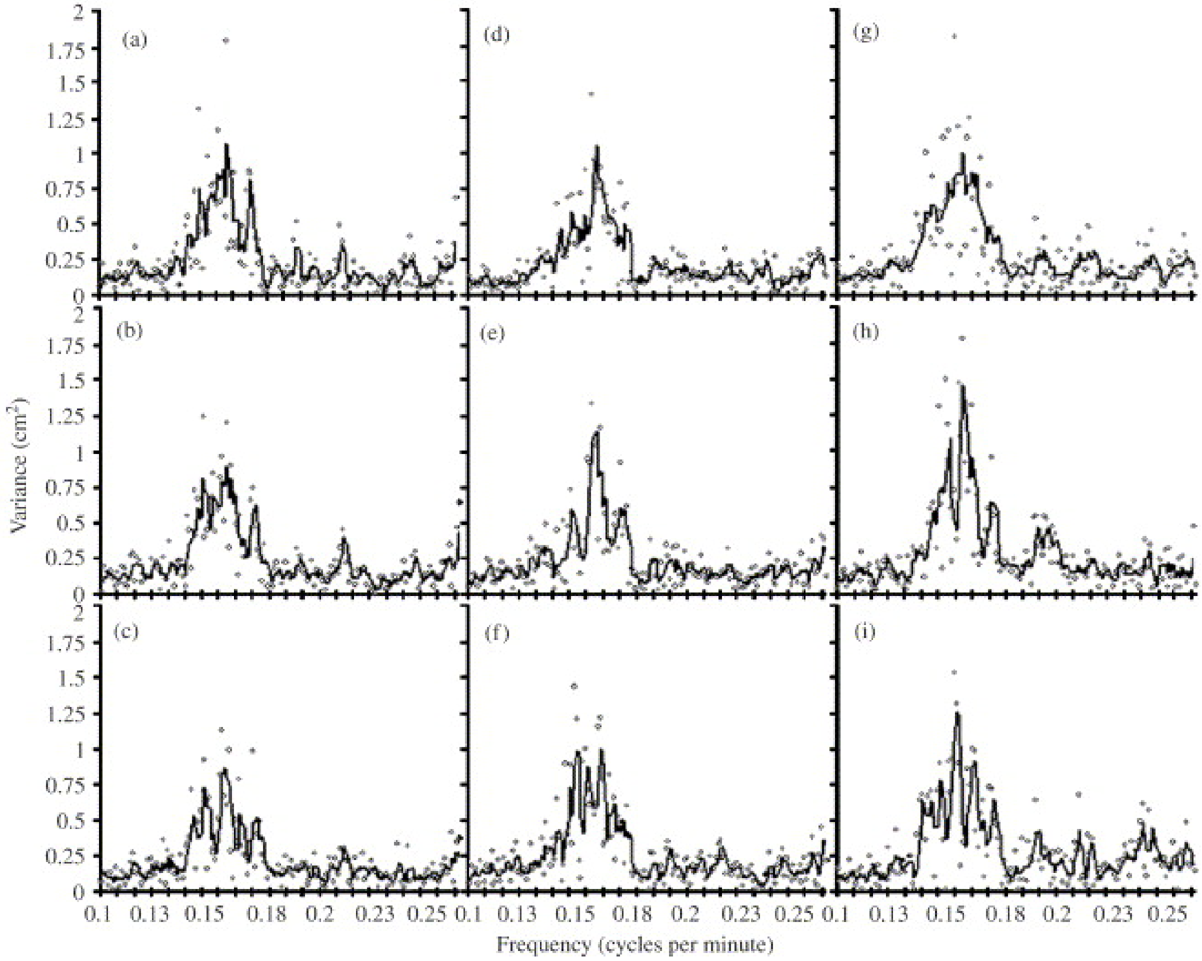

Fig. 6. An averaged of the 72 individual spectra (circles) (DoF=144, Emery and Thomson, 2001), showing the 95% confidence interval (dotted lines), for the time period beginning year day 154 (2004). The solid line represents a 3 point average.

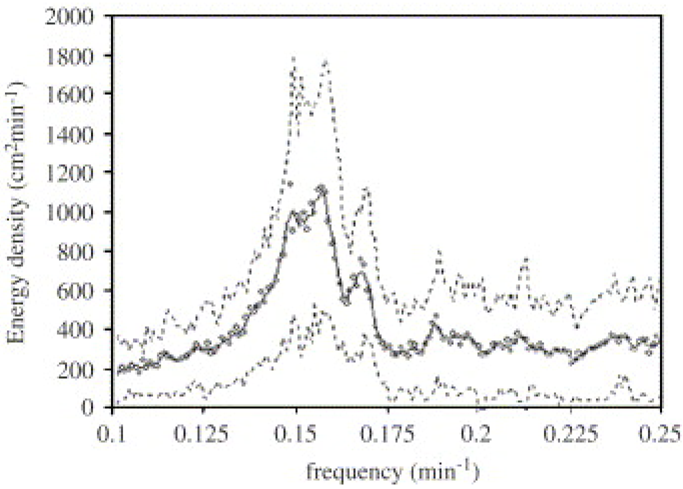

Fig. 7. Results from a wavelet analysis of about 33 h beginning at year day 160 (2004): (a) residual sea-level data; (b) wavelet power spectra; and (c) global wavelet showing the time averaged frequency spectra. The predicted spread of the fundamental mode is shown by the dashed lines on (b).